

XPS study of pulsed laser deposited CN_x films

F. Le Normand,^{1,*} J. Hommet,¹ T. Szörényi,^{2,3} C. Fuchs,² and E. Fogarassy²
¹IPCMS-GSI, UMR 7504 CNRS, Boîte Postale 20, 67037 Strasbourg Cedex 2, France
²CNRS-PHASE, UPR 292 CNRS, Boîte Postale 20, 67037 Strasbourg Cedex 2, France
³Research Group on Laser Physics, 6701, P.O. Box 406, Szeged, Hungary
 (Received 27 November 2000; published 28 November 2001)

The C 1s and N 1s core levels of carbon nitrides are composed of several contributions whose assignment is controversial due to the lack of appropriate reference materials and the great variety of configurations of carbon and nitrogen. From the comparison of nitrogen-containing polymeric compounds and solid carbon references an assignment of the individual lines of the C 1s and N 1s core levels is given. Nitrogen-containing polymeric compounds are used as reference materials as they provide a more adequate account of the screening of the ionized states in the photoemission process than molecular references. This screening effect is even more pronounced in case of aromatic or cyanogen-type bonds where delocalized π electrons strongly affect the screening of the core hole. In the second part of the paper these assignments are used to interpret the changes of the chemical environment in pulsed laser deposited carbon nitride films as a result of systematic changes in laser fluence, nitrogen pressure, and target-to-substrate distance. The effect of subsequent annealing and sputtering by argon ions is also discussed. The chemical structure of the films is dominated by nitrile, N(pyramidal)-C(trigonal) and nitrogen in sp^2 hybridization (with the electron doublet out of plane) inserted into carbon graphitic network at high laser fluence, and nitrile and pyridinic sp^2 -hybridized configurations at low laser fluence, in good line with the fact that sp^3 and sp^2 hybridization states around carbon and nitrile configuration with nitrogen, are preferred.

DOI: 10.1103/PhysRevB.64.235416

PACS number(s): 61.48.+c, 81.15.Gh

I. INTRODUCTION

The theoretical prediction of Liu and Cohen¹⁻³ on the existence and the expected outstanding properties of the covalent β - C_3N_4 , followed by further theoretical studies⁴ triggered many experimental efforts on the synthesis of this hypothetical material. Mentioning only the few, hot filament chemical vapor deposition,⁵⁻⁷ plasma-enhanced chemical-vapor deposition (PECVD),^{8,9} reactive rf sputtering,^{10,11} dc magnetron sputtering,^{12,13} ion beam assisted sputtering,¹⁴⁻¹⁶ laser ablation,¹⁶ and reactive ion implantation¹⁷ were implemented to grow thin carbon nitride films. More than 70 papers report the synthesis of C_3N_4 in different crystalline forms, but as revealed by a recent critical review in Matsu-moto, Xie, and Izumi,¹⁸ no definite evidence for the existence of C_3N_4 has ever been presented. Beyond the strong efforts to achieve the stoichiometric compound, the preparation of amorphous CN_x ($0 < x < 1.33$) films has emerged as a challenge, as these materials also display many interesting properties. In the overwhelming majority of the cases reported no more than 50 at. % of nitrogen has been incorporated into carbon films in the amorphous state, which still remains far from the stoichiometry corresponding to the β - C_3N_4 phase (57 at. %). For both types of compounds, there is a need to prepare more homogeneous films for more convincing structural characterizations, which requires first a deeper investigation of the parameters of the formation of a carbon-nitrogen bond in a solid. In addition to structural investigations by selected area diffraction or x-ray diffraction, X-ray photoelectron spectroscopy (XPS) emerged as a powerful tool to provide surface information on the local environment around both carbon and nitrogen, and indeed XPS was routinely used to determine the surface chemical com-

position (most notably the N/C XPS ratio) of carbon nitride films. However, the presence of many possible local environments and the lack of proper references have introduced some controversy into the interpretation of the individual contributions of the C 1s and N 1s core levels (e.g., Refs. 13, 14, 19 and references therein).

Here we present an XPS study of carbon nitride films prepared by pulsed laser deposition (PLD). These films have otherwise been characterized by infrared (IR), Raman, and photoluminescence spectroscopies together with an optical emission spectroscopic study of the gas phase processes.²⁰⁻²² The paper is organized as follows: After this Introduction the experimental procedures are first reviewed: details of film preparation and the XPS analyses are presented (Sec. II). In Sec. III an assignment of the individual lines of the C 1s and N 1s core levels is given as a result of a comparative analysis of binding energies of carbon-carbon and carbon-nitrogen bonds in solid carbon references and polymeric compounds containing both carbon and nitrogen. The effects of the process parameters and posttreatments on the chemical composition of the films are reported in Sec. IV together with the changes in the chemical environment of the carbon and nitrogen atoms. The interpretation and the evolution of the chemical structure of the films as a function of process parameters is discussed in Sec. V in comparison with literature data. Finally, conclusions are drawn in Sec. VI.

II. EXPERIMENTAL PART

A. Film preparation and post-treatments

Carbon nitride films were deposited in a conventional PLD system by ablating a high-purity graphite target in static

nitrogen atmosphere. The deposition chamber was pumped by a diffusion pump, with a base pressure $< 10^{-6}$ mbar, and back filled with 0.01–5 mbar N_2 during the experiments. The beam of the ArF excimer laser (Lambda Physik, $\lambda = 193$ nm, output energy max. 240 mJ, 22 ns pulse duration) was focused onto the target surface at normal incidence. The target was rotated with 1 rpm. The energy density on the target surface, Φ was adjusted between 4 and 18 J/cm² by changing both the output energy of the laser and the dimensions of the ablated area. Due to uncertainties in measuring both the pulse energy and spot dimensions, the experimental error in the absolute value of the energy densities was quoted to $\pm 20\%$ at best. Films of 50–300 nm thickness were deposited on *n*-type Si(100) wafers held at room temperature, at target-to-substrate distances d between 30 and 70 mm and 80 Hz pulse repetition rate.

Some samples were sputtered by argon ions or annealed in a ultrahigh vacuum chamber before XPS analysis. The sputtering conditions were: $p = 3 \times 10^{-5}$ mbar, ion energy = 800 eV, and an incidence angle of the ions with the surface of around 40°.

B. X-ray photoelectron spectroscopy (XPS)

The XPS spectra were recorded with a VSWTM spectrometer equipped with a 150 mm electron analyzer using a channel-plate detection mode. A monochromatic AlK _{α} radiation source provided a photon beam of $h\nu = 1486.6$ eV. The analyzer was operated in the fixed analyzer transmission mode at a constant pass energy of 22 eV. The experimental resolution, including the source and the analyzer, was set at 0.75 eV, measured by the broadening of the 4f7/2 line of a gold foil. Sets of C 1s, N 1s, O 1s, F 1s core level spectra as well as wide scans were recorded.

The energy levels were referenced to the Au 4f7/2, Ag 3d5/2, and Ag M₄N₅N₅ Auger lines at 83.98, 368.26, and 1129.79 eV, respectively. Charge effects due to the insulating character of the films were partly compensated by an electron gun. The energies were referred to the C 1s line A at 284.6 eV, as discussed later.

Since the films were amorphous, all the carbon-carbon and carbon-nitrogen bonds were statistically distributed on the surface and therefore the C 1s and N 1s levels had to be treated as a whole. The atomic ratio of nitrogen over carbon, (N/C), could be expressed from the classical formula of photoelectron spectroscopy²³

$$(N/C) = (I_N/I_C) \left[\left\{ \frac{T(E_k^C)}{T(E_k^N)} \right\} \left[\frac{\lambda(E_k^C)}{\lambda(E_k^N)} \right] (\sigma_C/\sigma_N) \right]. \quad (1)$$

In Eq. (1) the recorded intensities of the N 1s and C 1s lines, I_N and I_C respectively, are corrected for the atomic photoionization cross sections σ_N and σ_C , the ratio of the transmission functions of the analyzer $T(E_k^C)/T(E_k^N)$ and the ratio of the attenuation lengths inside the material $\lambda(E_k^C)/\lambda(E_k^N)$, where E_k^C and E_k^N were the kinetic energies at the C 1s and N 1s core levels, respectively. $\sigma_C/\sigma_N \approx 0.56$ (Ref. 24) and $T(E_k^C)/T(E_k^N)$ was experimentally determined

to be ≈ 1 . Unfortunately the ratio $\lambda(E_k^N)/\lambda(E_k^C)$ was hard to determine in amorphous carbon nitrides. The attenuation lengths depended not only on the kinetic energies and on the atomic number,²⁵ but also on the atomic densities inside the material. Now the density of the films changed with changing process parameters. Since the energy of the bulk plasmon on the C 1s level was directly proportional to the density of the valence electrons around carbon, electron-energy-loss spectroscopy (EELS) was used to monitor the changes in the atomic density of the films.²⁶ In this study, the bulk plasmon energy on the C 1s level shifted from 26.5 to 28.4 eV when increasing the laser fluence from 4 to 13 J/cm², suggesting an increase from medium to high valence electron density around carbon. In our calculations we assumed that $\lambda(E_k^C)/\lambda(E_k^N) \approx 1$, as the electron energies and the atomic numbers were in a close range, but this assumption might introduce an error that could be estimated to be no more than 15%. Another source of error was the *ex situ* adsorption of adventitious carbon leading to an underestimation of the N/C ratio. The extent of this error was hard to estimate, nevertheless it could be assumed this was a rather constant and systematic error.

In conclusion, the (N/C) ratio as calculated according to Eq. (1) yields only an estimate of the absolute value of the atomic ratio (N/C)_{at}. However, even if the XPS measurements reported here might inaccurately give the true atomic surface compositions, the changes in the (N/C) ratio correctly follow the evolution of the true (N/C)_{at} ratio as a function of the process parameters.

Lineshape analyses of the individual C 1s and N 1s lines were carried out using a home-made software. The data were first smoothed and subsequently deconvoluted including both a gaussian broadening accounting for the experimental resolution, electron-phonon interaction and amorphization effects, as well as a lorentzian broadening accounting for the lifetime of the core hole fixed to 0.21 eV for both the C 1s and N 1s lines. An inelastic Shirley form was postulated and added to each individual elastic contribution of the photoemission process.²⁷ In the fitting procedure the lorentzian broadening, which was an atomic property of the element, was let fixed whereas the energy position, the intensity of each individual contribution and the overall gaussian broadening were made variable. For n contributions ($n = 2$ or 3), this yield $2n + 1$ (5 or 7) fitting parameters for a peak made up of N points. With an energy step of 0.05 eV and a full width at half maximum of 1.2 eV, the individual components were composed of around 25 experimental points, ensuring $n \times N \gg 2 \times (2n + 1)$. In fact, only those fitting parameters that were believed not to be too strongly correlated were allowed to vary together, such as the energy position of one contribution i and the intensity of another one j . This ensured that the fit converged with the best probability toward the unique solution. It was reassuring to note that when starting from intentionally different initial parameters and using different sets of fitting parameters, the fit converged toward the same solution, constituting further proof to the uniqueness of the solution. Our conclusion was that, within the limits of the experimental resolution that was not better than 0.75 eV, the

results of the deconvolution of the C $1s$ and the N $1s$ levels into individual lines were physically sound.

III. INTERPRETATION OF THE INDIVIDUAL C $1s$ AND N $1s$ LINES

Figures 1 and 2 display the evolution of C $1s$ and N $1s$ core level spectra, respectively, with processing laser fluence Φ . The experimental spectra are fitted with a combination of three and two contributions to the C $1s$ and N $1s$ lines, respectively. In our case attempts to put more than three lines on the C $1s$ core level or more than two lines on the N $1s$ core level, respectively, did not improve the fit. It was sometimes possible to add one more line on the C $1s$ core level at higher binding energy. This fourth line accounts for a C-O contribution shifted toward high binding energy due to the high polarization of the C-O bond. But even if this contribution does exist, it remains weak and weakly overlaps the main C—C and C—N contributions, therefore it will be ignored in the following discussion. Wide scans displayed, in addition to carbon and nitrogen, oxygen and fluorine as impurities. The origin of this fluorine impurity, whose concentration increased with the laser fluence, remained unclear. It could either come from the graphite target or, more probably, from the pump oil.

Carbon as well as nitrogen possess many bonding configurations. Among the possible configurations of carbon, the tetrahedral (*tetra*), the trigonal (*tri*), and the linear (*lin*) configurations, which correspond to the sp^3 , sp^2 , and sp hybridization states, respectively, are the most commonly encountered. The sp^2 configuration may involve a pair of carbon atoms with a lone π bond, such as in alkenes, or conjugated π bonds involving many pairs of conjugated carbon atoms in conjugated π bonds. In this last case a significant decrease of the bonding energy occurs, like the aromatic bond in cyclized planar compounds. Other possible configurations, such as those involving a nearly conjugated sp^2 configuration in fullerene-like compounds, will not be considered in our analysis. Nitrogen atoms possess much more bonding configurations, due to the occurrence of the free doublet that can either participate or not to the bond. Besides the terminal collinear (*col*) nitrile bond illustrated by Polyacrylonitrile (PAN) in Table I and the sp^3 hybridization with σ bonds in a pyramidal (*pyr*) configuration like Polyethyleneimine (PEI), we must distinguish among nitrogens with sp^2 hybridization involved into aromatic carbon cycles, either as pyridiniclike in Poly(4-vinylpyridine) (P4VP in Table I) or as pyrroliclike in Poly(9-vinylcarbazole) (P9VC in Table I) trigonal configurations (sp^2 IP and sp^2 OP, respectively). We can note that pyridinic nitrogen cannot be inserted into a graphitic network as the free doublet is in an in-plane direction, but pyrrolic nitrogen can be inserted as the free electron doublet participates to the aromatic configuration.²⁸

In Table I binding energies of carbon-carbon and carbon-nitrogen bonds in selected solid state and polymeric compounds are compiled including the bonding configuration on each atom. We have chosen solids^{29,31,32} or, when these are lacking, polymeric references from the same data set of the literature³⁰ as they best simulate the initial- and final-state

effects in the XPS process that will be further discussed. We discarded molecular compounds such as pyridine, hexamethylenetriamine, urotropine or other pure organic molecules, often referred to in the XPS analysis of CN_x films,^{14–19} since these materials can neither satisfactorily account for the initial-state (charge transfer) nor the final-state (screening of the core hole by electrons) effects of the core level shift, especially when considering π -conjugated systems. The reference to the carbon solid state is graphite (*G*) at 284.6 eV (Ref. 29) and to the polymer state aliphatic carbon of polyethylene [high-density polyethylene (HDPE)] at 285.1 eV,³⁰ respectively. We consider these two sets of references to be consistent, as the aromatic carbon in poly(α -methylstyrene) P α MS (set in position 1 in Table I) is shifted by -0.34 eV as compared to the aliphatic carbon (set in position 2), in good agreement with the difference of -0.5 eV found between the binding energies [(*G*)-(HDPE)] (Table I). When comparing now diamond (C $1s=285.6$ eV) and polyethylene (HDPE) (C $1s=285.1$ eV) as solid state and polymer references of the C(tetra)—C(tetra) bond, respectively, we find a difference of 0.5 eV. As both the near neighbors of carbon (C, C and H, respectively) and the atomic densities (high and low, respectively) are different, this 0.5-eV difference is realistic and defines the accuracy limits of the method described above. Moreover, the energy position of the C $1s$ peak of diamond is influenced by the surface reconstruction or the doping level. A band bending at the surface, which is induced by a deviation of the charge density at the surface as compared to the bulk and therefore a pinning of the Fermi level at a different position within the gap, may lead to a shift of the C $1s$ peak. Therefore we also include the reference of a tetrahedrally coordinated amorphous carbon *aC*.³² When dealing with the carbon-to-nitrogen bond, we report in Table I a reference polymer for both the carbon-nitrogen and the equivalent carbon-carbon bond. A carbon atom is defined to be in an equivalent configuration to a nitrogen atom when the same amount of π bonds is involved in the carbon-carbon and the carbon-nitrogen bonds. Hence tetrahedral, trigonal, and linear carbon bond configurations are equivalent to pyramidal, sp^2 -hybridized either in- or out of plane, and terminal collinear nitrogen bond configurations, both involving 0, 1, and 2π bonds, respectively. The difference δ between the C $1s$ core level of the carbon bound to nitrogen and the carbon bound to an equivalent carbon is also reported in Table I for these reference compounds. For example when comparing HDPE and polyethyleneimine (PEI), the carbon atom in tetragonal configuration bonded to another tetragonal carbon in HDPE or to nitrogen in pyramidal configuration in PEI exhibits binding energies at 285.10 and 285.56 eV, respectively. This means that the substitution of carbon by nitrogen in an equivalent configuration yields a positive shift $\delta=0.46$ eV. The column entitled Ref. (C—N)—(C—C) displays the references used in the determination of δ . In the last column of Table I the binding energies E_B , corrected with reference to carbon in graphite at 284.6 eV, are compiled for different carbon-carbon and carbon-nitrogen bond configurations. In the following, δ and E_B will

TABLE I. XPS binding energies of carbon-carbon and carbon (boron)-nitrogen bonds in reference solid state (*S*) and polymer (*P*) compounds. The energy references are 284.6 eV for solid state references (Refs. 29 and 31) and 285.0 eV for polymer compounds (Ref. 30). C(tetra), C(B)(tri), C(lin) refer to carbon in the tetrahedral, trigonal, and linear configurations, respectively. N(pyr), N(sp^2 IP), N(sp^2 OP) and N(col) refer to nitrogen in the pyramidal, in-plane sp^2 -hybridized and out of plane sp^2 -hybridized, and collinear configurations, respectively.

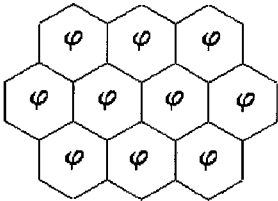
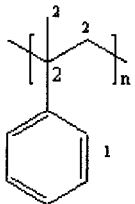
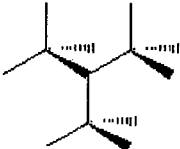
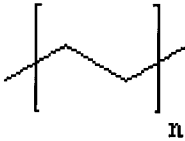
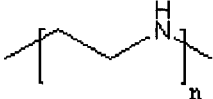
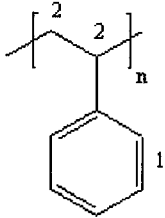
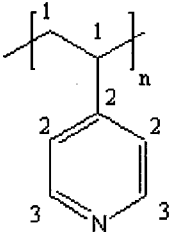
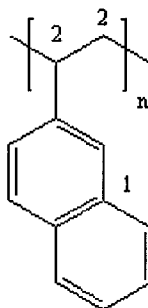
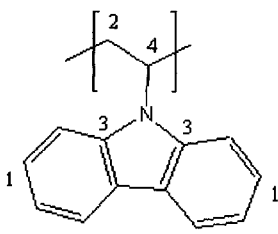
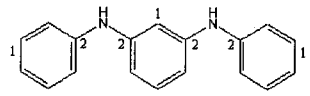
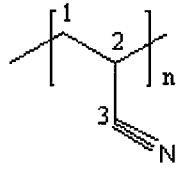
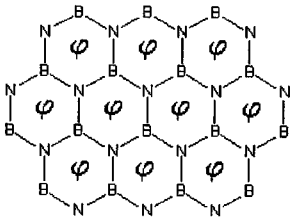
Bond type	References	Nature	Formula	C 1s (eV)	N 1s (eV)	δ (eV)	Ref. (C-N)- (C-C)	Δ (eV)	E_B (eV)
C(tri)-C(tri)	Graphite (G) [29]	S		284.60					284.60
C(tetra)-C(tri)	ta:C [32]	S	amorphous	284.44 285.25					
	Poly(α -methylstyrene) (P α MS) [30]	P		(1) 284.66 (2) 285.00					(1) 285.16 (2) 285.50
C(tetra)-C(tetra)	Diamond (D) [29]	S		285.60					285.60
	Polyethylene (HDPE) [30]	P		285.10					285.60
C(tetra)-N(pyr)	Polyethylenimine (PEI) [30]	P		285.56	399.07	0.46	PEI-HDPE	113.51	286.06
	Polystyrene (PS) [30]	P		(1) 284.76 (2) 285.00					(1) 285.26 (2) 285.50
C(tri)-N(sp^2 IP)	Poly(4-vinylpyridine) (P4VP) [30]	P		(1) 285.00 (2) 285.48 (3) 285.99	399.34	1.23	P4VP-PS	113.35	(3) 285.83

TABLE I. (Continued).

Bond type	References	Nature	Formula	C 1s (eV)	N 1s (eV)	δ (eV)	Ref. (C-N)- (C-C)	Δ (eV)	E_B (eV)
	Poly(2-vinylnaphthalene) (PVN) [30]	P		(1) 284.76 (2) 285.00					
C(tri)-N(sp ² OP)	Poly(9-vinylcarbazole) (P9VC) [30]	P		(1) 284.67 (2) 285.00 (3) 285.61 (4) 286.41	400.22	0.95	P9VC- PαMS	C(tri)114.61 (3)285.55 C(tetr)113.81 (4)286.41	
C(tri)-N(pyr)	N,N'-Diphenyl-1,4- phenylenediamine [poly(aniline) oligomer] (PA) [30]	P		(1) 284.70 (2) 285.94	399.92	1.28	PA- PαMS	113.98	286.44
C(lin)-N(col)	Polyacrylonitrile (PAN) [30]	P		(1) 285.48 (2) 286.35 (3) 286.73	399.57	-	-	112.84	286.73
B(tri)-N(sp ² IP) (partial)	Boron nitride (hexagonal NB) [31]	S		-	397.90			113.0 ⁽¹⁾	

(1) $E_{N1s}(NB) - E_{C1s}(G)$

be derived in the light of existing theoretical interpretations of the binding energy shift of a core level. Based on these considerations the assignment of the individual lines of the C 1s and the N 1s levels will be given.

A. C 1s levels

The binding energy of the core level K of a photoelectron escaping the surface of a sample referenced to the vacuum

level, $E_b^{\text{vac}}(K)$, can be expressed in the general framework of the charge potential model:^{33,34}

$$E_b^{\text{vac}}(K) = E_{b,0}^{\text{vac}}(K) + k(K)q_i + \sum_{j \neq i} (q_j/r_{ij}) - E_{\text{relax}}(K), \quad (2)$$

where $E_{b,0}^{\text{vac}}(K)$ is the binding energy referred to the vacuum level of a reference state, which is generally equal to the binding energy of the core level of the atomic state according to Koopman's theorem; $k(K)q_i$ is a term of polarization of the bond where k is a two-electron integral between the core K and the valence electrons; $\sum_{j \neq i} (q_j/r_{ij})$ is the electrostatic potential of Madelung's-type accounting for the interaction of the environment that in the case of a covalent bond is proportional to the first neighbors, and $E_{\text{relax}}(K)$ encompasses the relaxation effects due to the core hole in the final state. This last multielectronic term stems from an interaction upon ionization of a core hole by the cloud of the valence band electrons. In Eq. (2) we assume that the work function is identical whatever the sample. Therefore this term is omitted throughout the text.

In the case of diamond and graphite where the bond involves identical atoms, there is no charge transfer at all, the intermediate terms $E_{\text{ICT}} = -k(K)q_i - \sum_{j \neq i} (q_j/r_{ij})$ cancel and Eq. (2) reduces to

$$E_b^{\text{vac}}(K) = E_{b,0}^{\text{vac}}(K) - E_{\text{relax}}(K), \quad (3)$$

where E_{ICT} is the energy of the initial charge transfer.

The chemical shift between diamond and graphite is therefore due to a difference in the relaxation energy of the two carbon electronic configurations. The four σ bonds in diamond are strongly oriented along the four directions of the tetrahedral arrangement, and therefore can hardly participate in the screening of the core hole. Conversely, the π bond can more easily be delocalized in conjugated or aromatic systems and therefore can more actively participate in the screening of the core hole. Indeed a line shift $\alpha = 1$ eV is reported in the competitive CVD growth of diamond islands and graphitic layers on Cu(111) [Ref. 29] (Table I). This 1 eV shift is also supported by recent literature data on the high-temperature graphitization of a diamond surface.³⁵

In the case of CN_x compounds, polarization occurs in the initial state, due to the difference of electronegativity between carbon and nitrogen atoms. Nitrogen has a greater electronegativity, therefore the electron cloud of the C—N covalent bonds tends to move toward the N atom.³⁶ This transfer of negative charges increases the binding energy of the C 1s level and decreases the binding energy of the N 1s level. It should be noted, however, that (i) the amplitude of the charge transfer is weak as the electronegativities of carbon and nitrogen are rather close but (ii) it increases with the number of C—N bonds due to the increasing polarization of the 1s electrons with increasing number of C—N bonds; (iii) this charge transfer is dependent on the nature of the bonding between carbon and nitrogen that can be of the amine-type N—C, imine- or aromatic-type N=C, or nitrile-type N≡C, and (iv) the polarization term $[k(K)q_i]$ in Eq. (2) is compensated by the electrostatic potential $[\sum_{j \neq i} (q_j/r_{ij})]$ due to the neighboring atoms. Applying Eq. (3) to carbon-carbon bonds

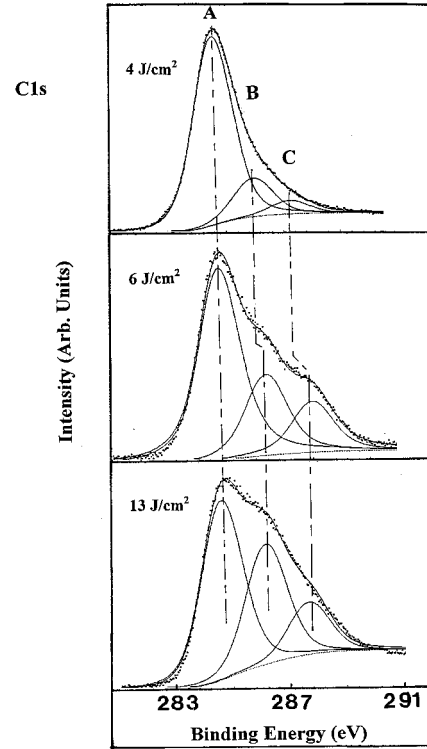


FIG. 1. Effect of the laser fluence on the C 1s core level of carbon nitride films deposited at $p=5$ mbar and $d=50$ mm. The points represent the experimental data while the solid lines the single contributions A, B, and C together with the overall fit. The assignment of the individual contributions is discussed in the text.

of configurations i and j , respectively (i and $j = sp^3$ or sp^2), and Eq. (2) to carbon-nitrogen bonds of equivalent configurations, the net shift in binding energy $\delta(\text{C}_i\text{-N}_j)$ due to substitution of a carbon C_j by a nitrogen N_j of equivalent configuration is

$$\delta(\text{C}_i\text{-N}_j) = kq_i + \sum_{k \neq i} (q_k/r_{ik}) + E_{\text{relax}}(\text{C}_i\text{-C}_j) - E_{\text{relax}}(\text{C}_i\text{-N}_j), \quad (4)$$

The absolute binding energies E_b (C 1s, $\text{C}_i\text{-N}_j$) for each $\text{C}_j\text{-N}_j$ configuration are obtained from the absolute binding energies of the respective $\text{C}_i\text{-C}_j$ configuration, $E_b(\text{C}_i\text{-C}_j)$, by

$$E_b(\text{C}_i\text{-N}_j) = E_b(\text{C}_i\text{-C}_j) + \delta(\text{C}_i\text{-N}_j). \quad (5)$$

In Table I the $\delta(\text{C}_i\text{-N}_j)$ values are also reported for various combinations of the carbon and nitrogen configuration states i and j . The $E_b(\text{C}_i\text{-C}_j)$ and $E_b(\text{C}_i\text{-N}_j)$ reported in the last column of Table I are deduced from the binding energies of graphite and diamond, and reference polymers (PaMS, PS,...). Comparing now the binding energy values obtained from the fit of the measured C 1s spectra with those compiled in Table I we propose the following assignment of the three main contributions to the C 1s core level:

(1) The line *A* at 284.6 eV is exclusively assigned to graphitic carbon i.e., graphiticlike or amorphous carbons in the films and adventitious carbon adsorbed on the surface. As the samples have been exposed to air prior to XPS analysis this last contribution must be accounted for. It is plausible, however, to assume that the extent of surface pollution is roughly constant from one sample to another, so that this contribution can be considered as a constant background to the signal.

(2) A close inspection of Table I suggests that the line *B* at around 286.0 ± 0.2 eV in Fig. 1 may be attributed to many bond configurations of carbon such as (i) diamond or diamondlike carbon and (ii) carbon singly bonded to nitrogen, either as a σ C—N or as a sp^2 hybridized π C=N bond, whatever the configuration of carbon is. All these bond energies range within 285.55–286.41 eV (Table I). Since this 0.86 eV range is of the same order as the experimental resolution (≥ 0.75 eV) we believe that it is hopeless to try to separate these contributions and only a global analysis is relevant. The small shift in the peak position with changing deposition conditions (Fig. 1) is probably due to variations in the relative proportions of each of these carbon-carbon and carbon-nitrogen contributions. The presence within the same C 1s line of many bonds is due to some compensation between charge transfer and relaxation effects on the core level of the positively charged carbon atom. In the π -type bond the transfer of charge to nitrogen increases, inferring a positive shift of the binding energy, but the screening of the core hole by the π electrons is more efficient, especially if these π electrons are delocalized, and this now infers a negative shift of the binding energy. On the other hand, the charge transfer to nitrogen is weaker in an σ -type bond, but the screening is also not so efficient due to the localized character of the σ electrons. Therefore the attribution of the 1.5 eV positive chemical shift relative to elemental graphiticlike carbon observed in contribution *B* cannot be explained in a simple way.

(3) Finally we assign the third line *C* at 287.2–287.7 eV to multiple σ C—N bonds such as the diamine (—CN₂—) bond. In this case the increase in the charge transfer shifts the line toward higher binding energies according to Eqs. (4) and (5). The charge transfer and screening, however, as both include long-range order effects, are nonlinear, i.e., are not strictly proportional to the number of C—N bonds. Unfortunately, in the absence of proper solid references or detailed quantum chemical calculations on the energy levels of the ionized atom, it is useless to speculate on a more accurate localization of this feature. Another possible assignment, however, might be nitrile-type triple bonds (—C≡N) and carbon linked to oxygen. A nitrile terminal bond is reported at 286.73 eV in Table I, not far from the binding energies of line *C*. It is expected that the terminal nitrile bond will not screen the core hole so efficiently than the other C—N bonds, due to a lower extent of screening in the former case. This is confirmed in Table I by the positive shift of the carbon in position 3 in the nitrile group of polyacrylonitrile (PAN) by 1.26 and 0.38 eV relative to aliphatic carbons in β (position 1) and α (position 2) of the nitrile group, respectively. The approximate 0.5 eV shift of contribution *C* with

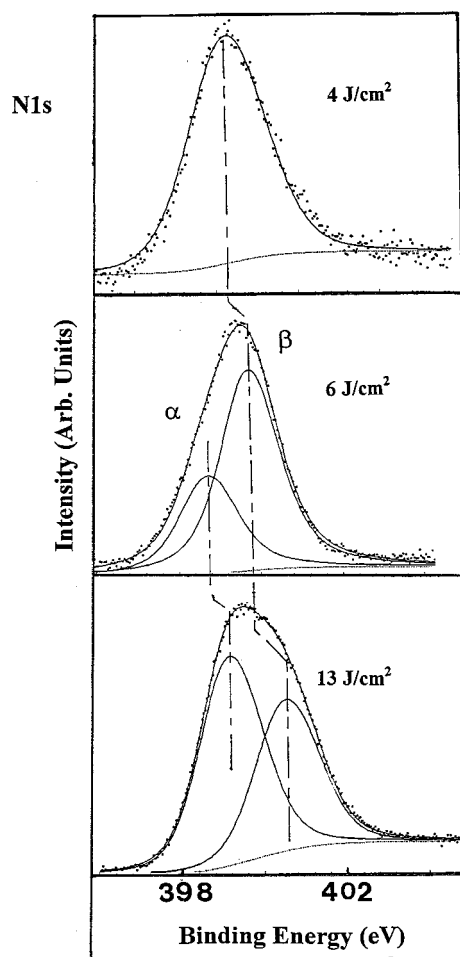


FIG. 2. Effect of the laser fluence on the N 1s core level of carbon nitride films deposited at $p=5$ mbar and $d=50$ mm. The points represent the experimental data while the solid lines the single contributions α and β together with the overall fit. The assignment of the individual contributions is discussed in the text.

increasing laser fluence (Fig. 1) is in line with the conclusion that more than one single chemical environment contribute to this feature, as well.

B. N 1s core levels

As shown in Fig. 2, the N 1s spectra display a double feature: a low binding energy component α at 398.8 ± 0.4 eV and a high binding energy one, β , at 400.0 ± 0.4 eV. The assignment of these N 1s peaks has long been discussed in the literature.^{13–15,19,37} Considering the N 1s binding energies of the polymers reported in Table I as references, we assign the low binding energy component α to unsaturated nitrogen in nitrile or pyridiniclike bonds. This assignment is based on the binding energy values of nitrogen in planar configuration such as poly(4-vinylpyridine) (P4VP) at 399.34 eV or collinear configuration such as PAN at 399.57 eV. However, the binding energy of the nitrogen-boron bond in hexagonal boron nitride, the unique solid nitride that may be relevant to the present study, is also very

low at 397.9 eV, although it exhibits a strong aromatic character with the free electron doublet. The shift toward low binding energy may be explained both by the larger negative charge transfer in the initial state as a consequence of the larger overlap of the π bonds and to the larger relaxation energy of the positively charged nitrogen atom in the final state. Changes in the contribution from different chemical environments around nitrogen with changing process parameters may explain the shift in the position of the line (Fig. 2). Lines at 398.0 ± 0.2 eV attributed to N-Si bonds^{31,38} might interfere with line α ; however, in our case any contribution from silicon bonds could be excluded because of the total absence of any Si2*p* signal in the wide scans.

We ascribe now line β at 400.0 eV to single N—C bonds with nitrogen in pyramidal configuration like *N,N'*-diphényl-1,4-phenylenediamine (PA) at 399.92 eV or to a π N-C bond of pyrrole-type with the free electron doublet out of the graphite plane like in P9VC at 400.22 eV (Table I). The positive shift in the binding energy is due to a weaker negative charge transfer in the initial state and to a weaker relaxation of the final state when σ single oriented bonds are involved. In P9VC the π electrons that could participate to the relaxation are transferred to the carbons nearby. On the other hand, lower binding energy has been measured for PEI where C(tetra)-N(pyr) bonds are involved. In the case of this reference, however, it is suspected that the presence of many terminal N-H bonds will markedly change the charge transfer and the relaxation effects. This global interpretation is in agreement with that put forward by Ronning *et al.*,¹⁹ but differs from many other one's.^{13–15} This point will be discussed in more detail in Sec. V.

In order to further support the assignments proposed above, let us consider now the difference in the binding energies of two neighboring carbon and nitrogen in a given configuration, $\Delta(N\ 1s-C\ 1s)$. According to Eq. (2)

$$\begin{aligned} \Delta(N\ 1s-C\ 1s) = & \Delta E_{b,0}^{\text{vac}}(N\ 1s-C\ 1s) \\ & + \Delta E_{\text{ICT}}(N\ 1s-C\ 1s) \\ & - \Delta E_{\text{relax}}(N\ 1s-C\ 1s), \end{aligned} \quad (6)$$

where $\Delta E_{b,0}^{\text{vac}}$, ΔE_{ICT} , and $\Delta E_{\text{relax}}(N\ 1s-C\ 1s)$ are the differences in the energy level reference, in the energy of the initial charge transfer, and in the relaxation energy between the N 1*s* and C 1*s* levels, respectively. These values sensitively depend on the initial charge transfer effect as the terms are of opposite signs on C and N atoms. Due to the electronegative character of nitrogen relative to carbon, there is a depletion and an enhancement in the electron density on carbon and nitrogen, respectively. Therefore the transfer terms add up in ΔE_{ICT} of Eq. (6). Conversely, the relaxation terms are subtracted, as—in a first approximation—the relaxation effect mainly depends on the cloud of delocalized π electrons and not on the nature of the atom to be screened.

In order to check the consistency of the proposed assignments, in Fig. 3 we plotted $\Delta(N\ 1s-C\ 1s)$ for the (α -*B*) and (β -*B*) line pairs as a function of the processing laser fluence and we compared these values with the $\Delta(N\ 1s-C\ 1s)$ values obtained for reference compounds (Table I). The expected

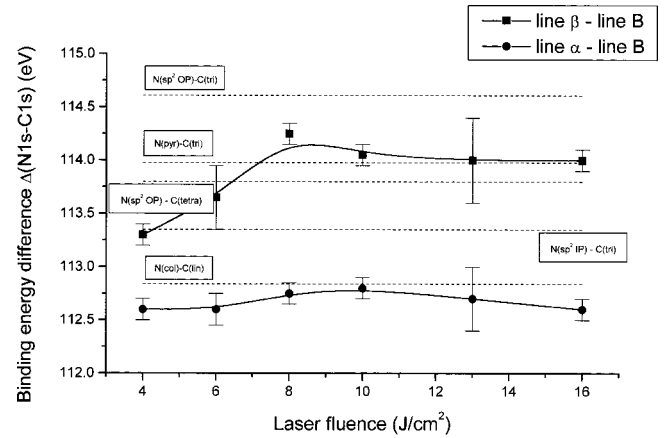


FIG. 3. Binding energy difference between the N 1*s* and the C 1*s* core levels $\Delta(N\ 1s-C\ 1s)$ corresponding to (α -*B*) (full circle) and (β -*B*) (full square) line pairs, respectively, as a function of the laser fluence for films deposited at $p=5$ mbar and $d=50$ mm. Dotted lines represent the binding energy corresponding to a given carbon-to-nitrogen configuration according to the references compiled in Table I.

range of $\Delta(N\ 1s-C\ 1s)$ variation does not exceed 2 eV. Although showing large variations with the laser fluence, the values of the (β -*B*) difference lie within the energy range expected for the N(sp^2 OP)—C(tetra) or N(pyr)—C(tri) configurations at high and the N(sp^2 -IP)—C(tri) configuration at low laser fluence (Table I). On the other hand the values of the (α -*B*) difference are characteristic of nitrile bonds. No other combination of the experimental N 1*s* and C 1*s* lines yield $\Delta(N\ 1s-C\ 1s)$ values consistent with the carbon-nitrogen configurations reported in Table I. This is especially true for combinations involving line A. References involving carbon multiply bonded to nitrogen are lacking. Therefore we do not consider line C in these combinations.

In summary, the corollary of the above comparative analysis is that the low binding energy component α may be assigned to nitrile rather than aromatic-type nitrogen bonds whereas the high binding energy component β may involve nitrogen in pyramidal or aromatic configurations, whatever the configuration of the carbon to which it is bonded. Nevertheless, large variations in the binding energies of these N 1*s* contributions are expected, owing to the variety of possible nitrogen configurations.

IV. EFFECT OF THE PLD PROCESS PARAMETERS

Pulsed laser deposition offers relatively easy control of film properties in a fairly broad range of process parameters. In the following the effects of the process parameters (laser fluence Φ , nitrogen pressure p , target-to-substrate distance d) and posttreatments (argon ion sputtering and thermal annealing) on the chemical composition of the films will be reported. Based on the assignments derived in the preceding section, changes in the chemical environment both around nitrogen and carbon atoms will also be detailed, as determined from the changes in the relative weight of the individual spectral components of the C 1*s* and N 1*s* lines.

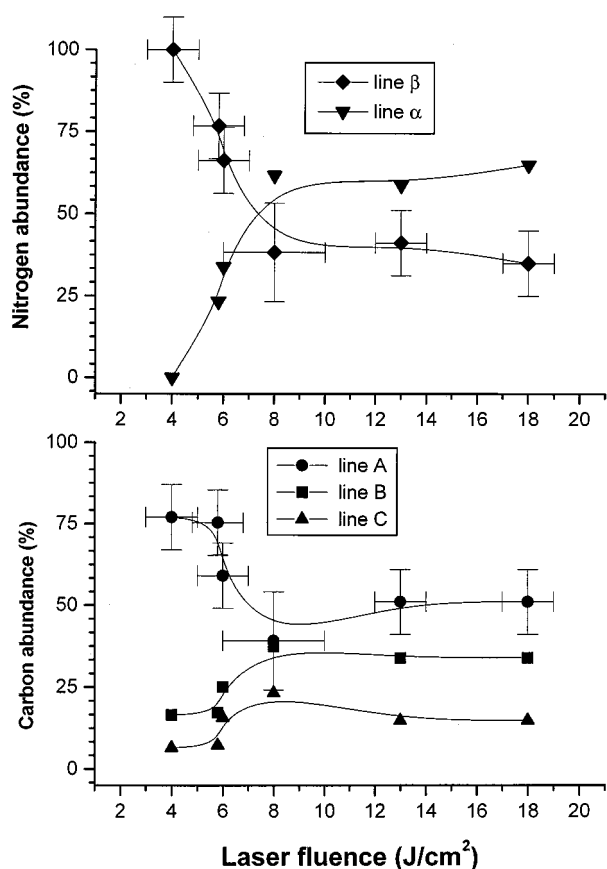


FIG. 4. Evolution of the relative abundance of the individual components of the N 1s and C 1s lines as a function of the laser fluence for films deposited at $p=5$ mbar and $d=50$ mm.

A. Effect of laser fluence

The amount of nitrogen incorporated into the films can sensitively be controlled by tuning the fluence of the ablating laser pulses. For 5 and 1 mbar similar dependences on fluence were obtained. The critical value is approximately 6–8 J/cm². The films deposited at 4 J/cm² contain only ≈ 9 at. % nitrogen. With increasing fluence the nitrogen content steeply increases, reaching ≈ 44 at. % at 8 J/cm² and the maximum value²² of ≈ 45 at. % at 10 J/cm². Further increase does not promote further incorporation of nitrogen atoms and above 10 J/cm² even a slight decrease is noticed.

Figures 4 and 5 display the changes in the relative abundance of the individual components of the C 1s and N 1s spectra as a function of laser fluence, for films deposited at a target-to-substrate distance d of 50 mm, $p=5$ and 1 mbar, respectively. Line A, corresponding to unsaturated carbon of graphitic type gives generally the major contribution to the C 1s spectra. At low fluence, the relative abundance of this contribution is 80%. In the 6–8 J/cm² fluence domain the intensity of line A drops leveling at around 40–50% above 8 J/cm². To the contrary, the initially weak lines B and C gain strength between 6 and 10 J/cm², suggesting that at these ablation pressures fluences larger than 6 J/cm² promote the formation of carbon-nitrogen bonds. Above 10 J/cm² changes in the fluence have apparently no further influence on the bond structure.

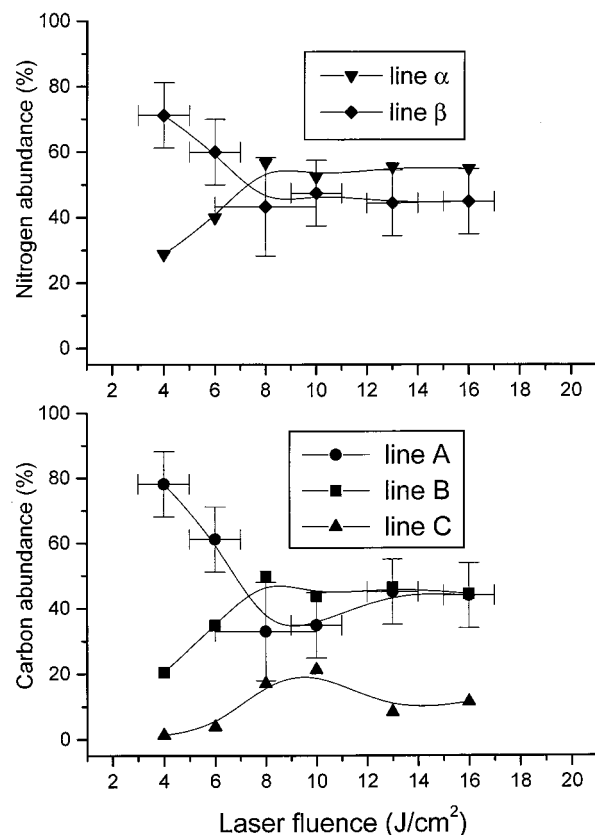


FIG. 5. Evolution of the relative abundance of the individual components of the N 1s and C 1s lines as a function of the laser fluence for films deposited at $p=1$ mbar and $d=50$ mm.

The changes in the relative weight of the two components of the N 1s spectra shown in Figs. 4 and 5 reveal that the laser fluence has an effect not only on the amount of nitrogen incorporated into the amorphous network, but also on the bond configuration of the nitrogen atoms. At 5 mbar and 4 J/cm² the N 1s spectrum can satisfactorily be fitted by a single line β while at 1 mbar the relative abundance of this line is ≈ 80 at. %. Accounting in addition on the $\Delta(N1s-C1s)$ values of the ($\beta-B$) difference (Fig. 3), we conclude that nitrogen atoms present in low concentration and at low fluence are first incorporated in a pyridiniclike configuration. With increasing nitrogen concentration more and more atoms form nitrile-, as reflected in the steep increase in the relative intensity of line α in proportion to β . In films deposited using fluences above 8 J/cm², the latter bond types become dominating, exceeding 60% relative abundance. This effect is more pronounced at high nitrogen pressures.

As shown in Figs. 1 and 2, the peak positions of components B and C of the C 1s core level and α and β of the N 1s core level spectra, respectively, shift to higher binding energies with increasing laser fluence. We consider this shift as a direct consequence of the contribution from different chemical environments to each of the lines. A closer inspection of Fig. 3 reveals that the ($\beta-B$) difference is the more affected. As both lines β and B encompass many carbon-to-nitrogen configurations, we cannot draw a definite conclusion. However N(pyr)-C(tri) and N(sp² OP)-C(tetra)

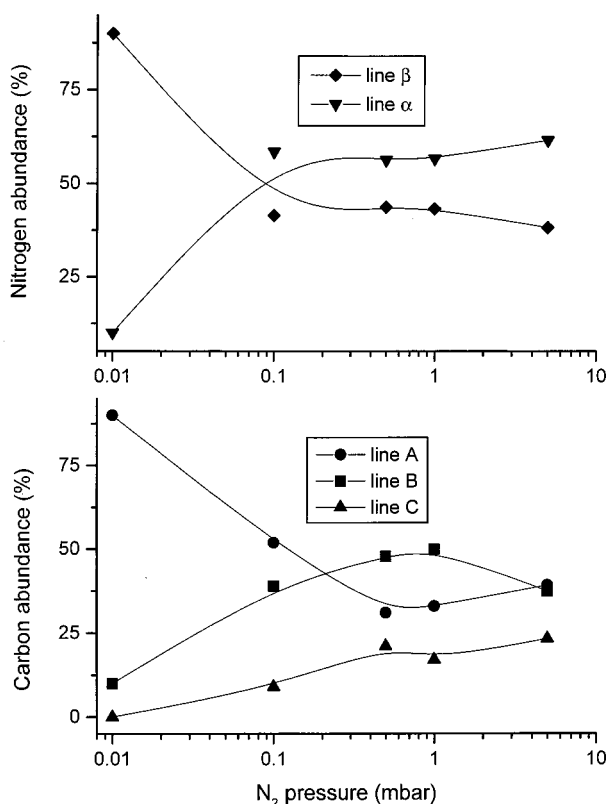


FIG. 6. Evolution of the relative abundance of the individual components of the N 1s and C 1s lines as a function of nitrogen pressure for films deposited at $\Phi = 8 \text{ J/cm}^2$ and $d = 50 \text{ mm}$.

configurations are now mostly expected. By contrast, the line α is less affected when changing the laser fluence. This suggests that the nitrile configuration is predominant.

B. Effect of nitrogen pressure

When ablating with pulses of medium fluences, i.e., $6\text{--}10 \text{ J/cm}^2$, nitrogen incorporation at at.% level starts at around 10^{-2} mbar. Between 10^{-2} and approximately 5×10^{-1} mbar the N/C ratio exponentially increases with increasing pressure, reaching a maximum with approximately 45 at.% nitrogen between 0.5 and 1.0 mbar. Further increase in pressure results in a slight decrease. Beyond 5 mbar a drastic decrease in deposition rate and powder formation hinder film formation.

Figure 6 shows the changes in the abundances of the individual components of the C 1s and N 1s core level spectra, as a function of nitrogen pressure. The laser fluence is $\Phi = 8 \text{ J/cm}^2$ and the target-to-substrate distance is $d = 50 \text{ mm}$. At low N₂ pressure component A dominates, as expected from the assignment of this line to a graphitic carbon-carbon bond exclusively. An increase in pressure from 10^{-2} to approximately 5×10^{-1} mbar results in a drop in component A, i.e., in the abundance of carbon atoms in pure graphitic environment, from $\approx 90\%$ to $\approx 30\%$. Concomitantly, component B, which is the measure of the number of carbon atoms in diamond like configuration and those connected to a single nitrogen atom, sharply increases. Our analysis suggests that

in films deposited under N₂ pressures between 0.5 and 1.0 mbar, half of the carbon atoms exists in these bonding configurations. Beyond 1 mbar the intensity ratio of components A and B shows an opposite behavior: whereas A slightly increases, component B decreases with increasing N₂ pressure. The turning point in both functions are exactly there where the nitrogen content of the films reaches its maximum value. This means that in a relative intensity vs nitrogen content (or N/C ratio) representation, the apparently biphasic character of both functions simplifies: component A decreases while B increases with increasing nitrogen content within the whole pressure domain investigated. The third component of the C 1s spectra, C, remains less significant. Its fraction, however, monotonously increases up to approximately 22% at 0.5 mbar, without noticeable changes beyond this pressure. All these experimental findings are consistent with the proposed assignments: with increasing nitrogen content the abundance of both components related to carbon-nitrogen bond configurations, B and C, increases at the expense of A. The contribution of C, assigned to multiple σ C—N bonds, becomes significant on samples deposited at the highest N₂ pressures only.

At the lower end of the pressure domain investigated, where the nitrogen concentration in the films is as low as 2 at.%, line β dominates the N 1s spectrum. At 10^{-2} mbar 90% of the few nitrogen atoms exists in pyramidal configuration bonded to sp^2 carbon. An increase in the N₂ pressure from 10^{-2} to 10^{-1} mbar results in dramatic changes not only in the absolute number of the nitrogen atoms incorporated into the network but also in the relative abundance of the bond types. While the total nitrogen concentration in the films increases from 2 to 31.5%, the contribution of line β falls from 90 to 41% with a concomitant increase in the relative intensity of line α from 10 to 59%, suggesting that the number of sites involving N atoms in nitrile-, pyridinic-type bonds increases much faster than the remaining nitrogen in pyramidal configuration or the incorporation of pyrrolic nitrogen. According to our analysis in the films grown at 10^{-1} mbar 19 at.% of the total atoms (considering N and C atoms only) exists in the former state, 13 at.% occupying sites of the latter configuration. At and above 10^{-1} mbar the relative abundance of both components remains constant. In terms of absolute values the concentration of nitrogen atoms corresponding to line α increases continuously throughout the whole pressure domain reaching 26 at.% at 5 mbar, while the number of nitrogen atoms corresponding to β line is maximum (at 19 at.%) in the films deposited at around 1 mbar.

The analysis of the $\Delta(\text{N } 1s - \text{C } 1s)$ differences further strengthens the soundness of the assignment of the individual C 1s and N 1s lines. From the (β -B) values at $114.2 \pm 0.1 \text{ eV}$ and (α -B) lines at $112.8 \pm 0.1 \text{ eV}$, respectively, the main carbon-to-nitrogen contributions can be assigned to N(pyr)—C(tri), N(sp^2 OP)—C(tri or tetra) and N(col)—C(lin) configurations (Fig. 7). The constant value of the differences suggests that the carbon-nitrogen configurations remain fairly stable when varying the nitrogen pressure, while keeping the laser fluence constant.

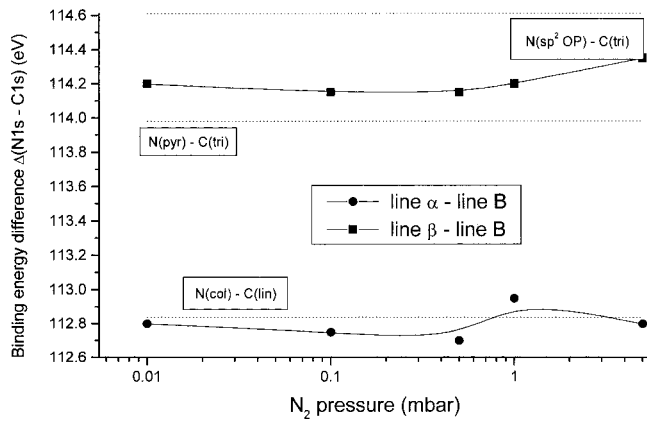


FIG. 7. Binding energy difference between the N 1s and the C 1s core levels $\Delta(N\ 1s - C\ 1s)$ corresponding to (α -B) (full circle) and (β -B) (full square) lines pairs, respectively, as a function of nitrogen pressure for films deposited at $\Phi = 8\text{ J/cm}^2$; $d = 50\text{ mm}$. Dotted lines represent the binding energy corresponding to a given carbon-to-nitrogen configuration according to the references compiled in Table I.

In summary we can state that within this domain of process parameters the nitrogen content tends to saturate at ≈ 45 at. %, implying an apparent stabilization of a stoichiometry near CN. Interestingly, the same limiting value (47–50 %) was reported for carbon nitride films grown by combining PLD with an atom beam as the nitrogen source,³⁹ instead of the N₂ atmosphere used in our experiments. The changes in the relative abundance of the individual components with nitrogen pressure reveal that incorporation of increasing amount of nitrogen atoms into the films results in characteristic changes in the local chemical environment of the majority of the carbon atoms.

C. Effect of target-to-substrate distance

The changes in both the C 1s and N 1s spectra of the films deposited at target-to-substrate distances between 30 and 70 mm are marginal in comparison with those due to changes in pressure and fluence. An increase in the distance from 30 to 70 mm results in less than 10% increase in the N/C ratio at 1 mbar and 10 J/cm^2 . Deposition at greater distances clearly promotes the incorporation of multiple σ C—N bonds as apparent from the monotonous increase in the abundance of line C of the C 1s spectra and line β of the N 1s spectra, respectively (Fig. 8). This result points to the importance of gas phase processes in determining the film composition: with increasing target-to-substrate distance, the probability of collisions of the ablated species with N₂ molecules in the gas phase and therefore the probability of incorporating nitrogen into the species impinging the surface increases. The $\Delta(N\ 1s - C\ 1s)$ differences calculated for the (β -B) and (α -B) line pairs are constant at 114.1 ± 0.1 and 112.55 ± 0.1 eV, again verifying that nitrogen atoms prefer pyramidal, sp^2 OP and nitrile configurations, respectively.

D. Effect of argon ion sputtering

As shown by the wide scans recorded on a film deposited at high laser fluence, sputtering by argon ions greatly influ-

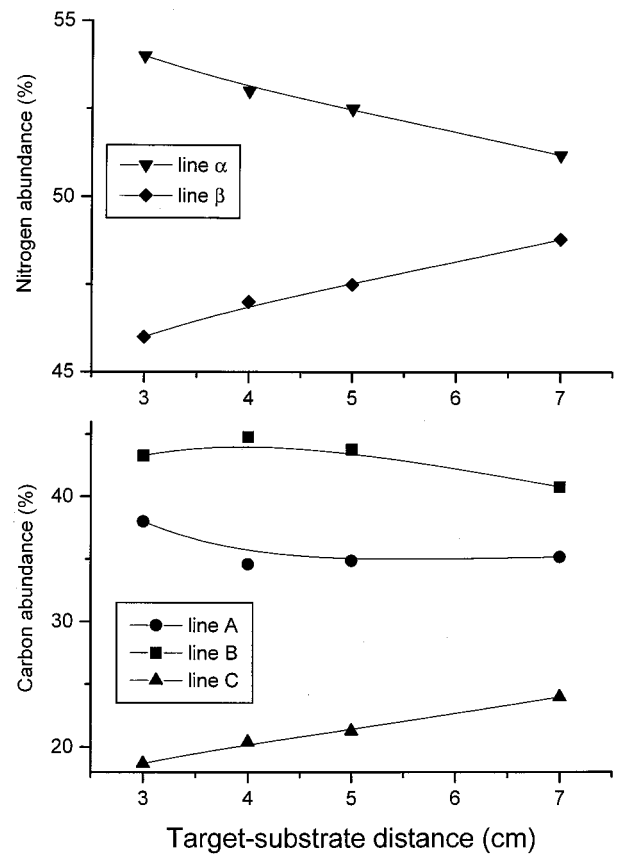


FIG. 8. Evolution of the relative abundance of the individual N 1s and C 1s lines as a function of the target-to-substrate distance d for films deposited at $\Phi = 10\text{ J/cm}^2$ and $p = 1\text{ mbar}$.

ences the overall intensity of the N 1s core level (Fig. 9), having apparently no effect on the relative abundance of each contribution of the N 1s core level (Table II). Concomitantly, the contributions B and C also become weaker (Fig. 10 and Table II), in line with the partial assignment of these lines to carbon singly or multiply bonded with nitrogen. However, it should also be noted that the ratio $B/(\alpha + \beta)$ increases with ion bombardment (Table II), despite the decreasing line B observed in Fig. 10. This again supports the assignment of contribution B not only to single carbon-nitrogen bonds but also to diamondlike carbon that is much hardly sputtered. The presence of additional diamondlike carbon is further evidenced by EELS spectra on the C 1s edge displaying a broad contribution around 28.4 eV that remains unchanged, and another one around 33.3 eV that can clearly be assigned to the bulk plasmon of diamondlike carbon (DLC not shown). These sputtering effects have been observed on samples deposited at different laser fluences and nitrogen pressures, and are in qualitative agreement with those reported by Bertóti and co-workers on the effect of Ar⁺, N₂⁺, He⁺ and H₂⁺ bombardment on chemical composition and structure of carbon nitride films of stoichiometry close to CN.⁴⁰ The ion sputtering reduces the oxygen and the fluorine concentrations, as well, suggesting that most of these impurities are weakly adsorbed.

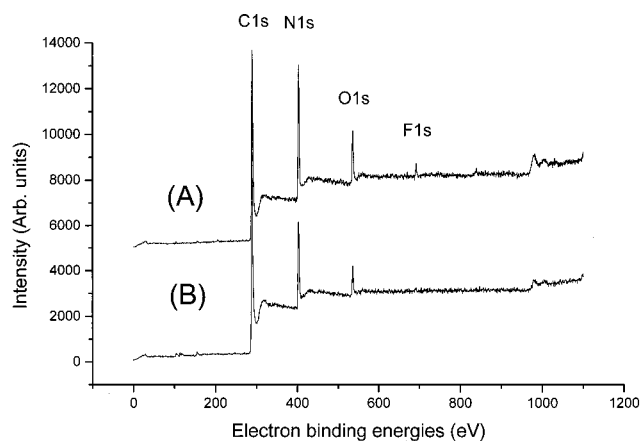


FIG. 9. XPS wide scans of films deposited at $p=5$ mbar; $d=50$ mm and $\Phi=13$ J/cm². (A) before and (B) after sputtering by argon ions.

E. Effect of vacuum annealing

The effects of thermal treatment at moderate temperatures are different from those of sputtering. The results of annealing of a film prepared at relatively high laser fluence ($\Phi=10$ J/cm²; $p=1$ mbar; $d=70$ mm) at 275 °C in vacuum are reported in Table II. Again the oxygen and fluorine contributions strongly decrease, while the intensity of the N 1s core level remains now practically not affected, revealing that the majority of the carbon-nitrogen bonds remains stable at this temperature. On the C 1s core level, no significant rearrangement in the relative abundance of the components can be obtained except the high-energy one, C. This finding can be explained by the easier removal of either some weakly bound C-O, multiple carbon-to-nitrogen bonds. The concomitant decrease in contribution β of the N 1s core level suggests, however, that the second explanation is the more plausible.

V. DISCUSSION

Although XPS has long been used as a routine technique for the characterization of carbon nitride films, there is still no agreement in the interpretation of the C 1s and N 1s core level spectra and therefore in the determination of the bonding around carbon and nitrogen. This is quite detrimental for correct predictions in the synthesis of such compounds. Vari-

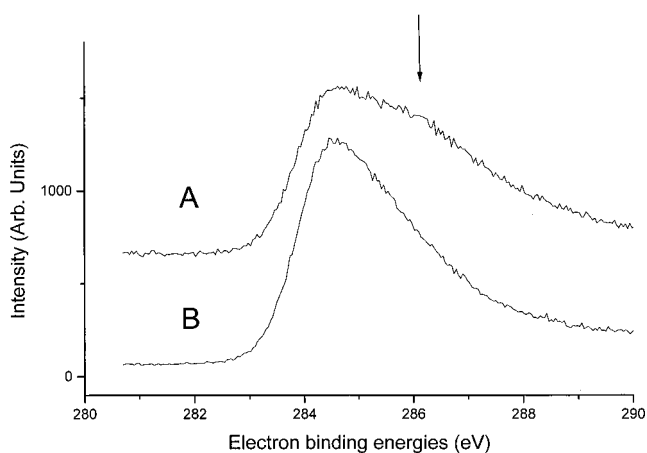


FIG. 10. C 1s core level spectra of a carbon nitride film deposited at $p=5$ mbar; $d=50$ mm and $\Phi=13$ J/cm². (A) before and (B) after sputtering by argon ions. The arrow indicates the position of line B in Fig. 1.

ous authors peak fitting procedure not only differs in the number of contributions they propose but also in the assignment of each component to chemical environments (Refs. 18, 19, 37, and references therein). The assignments put forward in this paper are in agreement with some reports, but at variance with some others. When comparing the different interpretations we focus on the reasoning used to settle the respective assignment.

Marton and co-workers¹⁴⁻¹⁵ assigned the N 1s high binding energy contribution β to nitrogen atoms bonded to sp^2 -hybridized carbon and the low binding energy contribution α to nitrogen atoms bonded to sp^3 -hybridized carbon. Their approach is based on a comparison with organic molecules containing nitrogen such as pyridine or hexamethylenetriamine. Such molecules might be considered as references of nitrogen in the single configurations N(sp^2 IP)—C(tri) and N(pyr)—C(tetra), respectively. Based on theoretical calculations and EELS measurements on the C 1s core level Sjostrom *et al.*¹³ and Ronning *et al.*¹⁹ suggested, however, an inverse assignment. Their results are also supported by the interpretation of the N 1s levels in 3,5,11,13-tetraazacycloazine, a molecule that contains nitrogens both in linear and pyramidal configurations.⁴¹ Our interpretation is in line with the latter assignments, except that,

TABLE II. Effect of the ion bombardment and *in vacuo* thermal treatment on the relative proportion of each individual C 1s and N 1s line.

		C 1s line (%)			N 1s line (%)		(C/N) _{at}	B/($\alpha + \beta$)
		A	B	C	α	β		
Ar ions bombardment	Before	51	34	15	59	41	1.9	0.65
	After	61	29	10	60	40	2.7	0.80
	Before	35	41	24	51	49	1.2	0.48
<i>In vacuo</i> annealing	After	41	44	16	60	40	1.1	0.50

based on the occurrence of an infrared signal corresponding to nitrile vibration at 2200 cm^{-1} , these late authors neglect the possible contribution of nitrile bonds to this line. Since the relative amplitude of the different carbon-nitrogen vibrations is not known and even strongly depends on the presence of conjugated carbons, we think that on the basis of IR and Raman measurements alone the contribution of nitrile bonds to the XPS spectra cannot be discarded. Muhl and Mendez³⁷ introduced the concept of mixing environment around nitrogen and carbon atoms, such as the one we have developed in this study, and they interpreted the different lines as governed by the charge transfer of the lone doublet on nitrogen that can widely vary according to the configuration of the surrounding carbon atoms. The shift of the peak is therefore governed by the charge transfer. They do not consider the screening of the ionized core hole.

The assignment of the three main lines *A*, *B*, and *C* of the C $1s$ core level also differs according to the authors. The interpretation of Ronning *et al.*¹⁹ considers that line *A* can be attributed to both any elemental carbon (diamondlike and graphiticlike carbons) and to sp^2 carbon linked to nitrogen whereas line *B* is attributed to sp^3 carbon-to-nitrogen bond and line *C* to tetrahedral carbon multiply bonded to nitrogen. Muhl and Mendez,³⁷ as well as Marton and co-workers^{14–15} partially accounting for the relaxation effects in the final state, put forward a completely different interpretation of the same features. They assign pure carbon to line *A*, and sp^2 carbon-nitrogen and sp^3 carbon-nitrogen bonds to line *B* and line *C*, respectively. Our interpretation is in line with Ref. 19 for line *C* and Ref. 37 for line *A* but differs from both for line *B* in the sense that we consider that more than one carbon bonding configuration can be assigned to the photoemission line merging from the fitting process around 286 eV. We believe that either the omission of the screening of the ionized atom or the consideration of organic molecules as references or the poor experimental resolution might explain the large variations in the interpretation of these individual lines. It is interesting to note the direction of the energy shift when the relaxation effects are not properly considered. If they are neglected this would induce according to expression (2) an upwards shift of the binding energies both on the C $1s$ and N $1s$ levels, as $E_{\text{relax}}(K) > 0$. Therefore strong variations of the absolute binding energy might be expected. This can be illustrated by the case of molecules and polymers both containing carbon and nitrogen atoms that are in the same configuration. The C $1s$ and N $1s$ binding energies in hexamethylenetetramine at 286.9 and 399.4 eV, respectively, quite differs from the values reported in polyethyleneimine (PEI) (285.56 and 399.07 eV, respectively) of the same C(tetra)-N(pyr) configuration. Hence large shifts occur between molecular and polymer compounds when no π electrons are involved in the carbon-nitrogen bond. The C $1s$ line shifts toward a higher binding energy in the molecule, indicating that the relaxation effect here is smaller than on the polymer. On the N $1s$ core level, smaller deviations are observed probably due to the presence of the lone doublet of electrons. By contrast the C $1s$ and N $1s$ binding energies in pyridine are 285.5 and 399.8 eV, respectively, to be compared with 285.99 and 399.35 eV in the polymer P4VP dis-

playing the same C(tri)-N(sp^2 IP) configuration. The effect is not so pronounced when π electrons are involved in the carbon to nitrogen bond.

Although continuously improving, the interpretation of the XPS features will remain essentially speculative until successful preparation of large area films of well-defined CN_x solid-state phases. Up to now only diffraction studies on small selected areas have been reported, but even the interpretation of the many patterns yet remained quite ambiguous.¹⁸ The reports upon XPS data on CN_x films display generally many contributions on both C $1s$ and N $1s$ lines, pointing to the presence of different configuration states of carbon and nitrogen coexisting in an amorphous matrix. No doubt, comparative studies on well-defined samples might help in improving the interpretation of XPS data, but perhaps it could be more instructive to compare our interpretation with XPS data recorded on samples where single lines are observed on both levels or with samples prepared at high temperature as better crystallized phases are expected. Among the few data that match these criterions, Woo *et al.*⁴² reported single C $1s$ contributions at 285.56 and 287.26 eV at relatively large (N/C \approx 0.36) and low (N/C \approx 0.16) nitrogen loading on CN_x films prepared by dc- and rf-plasma enhanced CVD at 1073 K, respectively. These lines were attributed to tetrahedral carbon coordinated to nitrogen and carbon in the nitrile bond, respectively. Unfortunately, the films were not fully covering the Si substrate and therefore some ambiguity still existed on the interpretation of the N $1s$ lines between N–C and N–Si species. Wu *et al.*¹¹ performed XPS analyses on rf CVD films prepared at around 773 K. They reported two lines on the N $1s$ lines instead of one line on the C $1s$ level at 286.5 eV that are attributable to some carbon-to-nitrogen bonds. The occurrence of one single line of the C $1s$ line indicated that many configuration states of carbon bonded to nitrogen would be included in this single line. Unfortunately, they neither reported the spectra nor they provided information about the spectral resolution. Matsumoto *et al.*⁴³ found by rf thermal plasma CVD at 823 K one single line on C $1s$ and N $1s$ levels at 285.25 and 400.0 eV, respectively, with a high N/C ratio of 1.43. However, the deposits showed powderlike texture and a low density due to large incorporation of hydrogen and oxygen. Moreover, many contributions were presumably hidden by the very broad width (\sim 4 eV) of the N $1s$ line. In conclusion, on a close inspection, literature on CN_x films prepared at high temperatures and characterized by XPS spectroscopy does not appear to be conclusive. This is due both to the difficulty in the high-temperature synthesis of CN_x films and to the poor resolution generally used in the XPS spectra. The difficulty to achieve CN_x films at high temperatures can be explained by the high etching rate of the plasma in presence of nitrogen and by the high volatility of the nitrile bond.

Another way to improve the local characterization around carbon and nitrogen in CN_x films is to perform X-ray absorption spectroscopy (XAS) in close addition to XPS. In XAS spectroscopy the ejected electron fills the lowest unoccupied states and as such are now participating in the relaxation process. Therefore it is reduced compared to XPS. The energy of the electron transition is given by an equation similar

TABLE III. Energy of the CC and CN bonds.

Bond type	Single		Double		Triple	
	C—C	C—N	C=C	C=N	C≡C	C≡N
Energy (kJ/mol)	347	305	611	615	837	891

to equation (2) but with a term $E_{\text{relax}}(K)$ that is reduced. Moreover, it is possible to separate the carbon and nitrogen in π states, corresponding to the $\pi \rightarrow \pi^*$ transitions from the σ states, corresponding to the $\sigma \rightarrow \sigma^*$ transitions. Finally, the technique is selective like XPS and with some precautions can be quantitative. Unfortunately, there are only a few XAS reports in the literature concerning CN_x films,^{12,44} using both XAS and XPS. The results are in good agreement and they strengthen our interpretation. However, the ambiguity concerning the nitrile contribution cannot be alleviated.

The results of the analysis outlined in the preceding section reveal that the nitrogen pressure and the laser fluence are obviously the two main parameters determining the chemical structure of the pulse laser deposited CN_x films. Their effects are, however, of different nature. Nitrogen incorporation is directly proportional to the nitrogen pressure up to approximately 1 mbar, while not much affecting the distribution of C—N bonds. To the contrary the dependence on laser fluence displays a thresholdlike behavior at 6–8 J/cm², affecting both the incorporation of nitrogen and the distribution of nitrogen-carbon bond configuration.

Examination of Figs. 1–5 points out rather large variations of respective concentrations in the carbon and nitrogen species. Bearing in mind the assignment of carbon and nitrogen contributions presented above, we can consider two domains as a function of the laser fluence. At low laser fluence the content of multiply bonded carbon is rather high but it decreases up to near 6 J/cm². We assign this line to π -delocalized carbon in graphiticlike network with some nitrogen incorporation into the aromatic carbon cycles. On the contrary in the high-fluence range (above around 10 J/cm²) the dissociation rate of nitrogen will be significantly enhanced. We expect that now simple C—N bonds, in substitutional position in a DLC carbon framework, and nitrile bonds are formed. It is believed, however, that the surface process is predominant as the species impinge the surface with a high energy and therefore the process is more or less

governed by the thermodynamics, the more at the highest fluence. A simple look at the relative stability of C—C and C—N bonds reported in Table III suggests that the triple bond C≡N is more stable than C≡C bond by 55 kJ/mol while the double C=C and C=N have equal stability and the single C—C bond is more stable than C—N bond by 40 kJ/mol.²⁸ Therefore it is expected that the nitrile configuration will predominate over the formation of simple or multiple C—N bonds. These trends are in good agreement with *ab initio* based tight-binding molecular dynamics calculations where the formation of paracyanogenlike structures is increased with nitrogen incorporation⁴⁵ and the lowering of the hardness on the films with a high nitrogen content.⁴⁶

VI. CONCLUSIONS

From the comparison of nitrogen-containing polymeric compounds and solid carbon references an assignment of the individual lines of the XPS C 1s and N 1s core levels of carbon nitride films grown by pulsed laser deposition is given. These assignments are used to interpret the changes in the chemical structure of the films as a result of systematic changes in process parameters (laser fluence, nitrogen pressure, and target-to-substrate distance), subsequent annealing and sputtering by argon ions. Albeit there are some evidence of nitrogen incorporation into carbon graphiticlike network, the formation of nitrile group is dominant as soon as the nitrogen-to-carbon atomic ratio increases. The N(pyramidal)—C(tetrahedral) multiple bond configuration characteristic of cubic C_3N_4 cannot unambiguously be determined from XPS analyses. Better spectral resolution together with binding energy calculations, as well as improvement in the preparation techniques and comparative characterizations are required to reach this goal.

ACKNOWLEDGMENT

Many thanks are due to Professor J.F. Nicoud (IPCMS-GMO, Strasbourg) for helpful discussion.

*Author to whom correspondence should be addressed.

¹A. Y. Liu and M. L. Cohen, *Science* **245**, 841 (1989).

²A. Y. Liu and M. L. Cohen, *Phys. Rev. B* **41**, 10 727 (1990).

³A. Y. Liu and R. M. Wentzcovitch, *Phys. Rev. B* **50**, 10 362 (1994).

⁴D. M. Teter and R. J. Hemley, *Science* **271**, 53 (1996).

⁵Y. Zhang, Z. Zhou, and H. Li, *Appl. Phys. Lett.* **68**, 634 (1995).

⁶P. H. Fang, *Appl. Phys. Lett.* **69**, 136 (1996).

⁷Y. Chen, L. Guo, and E. G. Wang, *Philos. Mag. Lett.* **75**, 155 (1997).

⁸T. Y. Yen and C. P. Chou, *Solid State Commun.* **95**, 281 (1995).

⁹S. Veprek, J. Weidmann, and F. Glatz, *J. Vac. Sci. Technol. A* **13**, 2914 (1995).

¹⁰K. M. Yu, M. L. Cohen, E. E. Haller, W. L. Hansen, and J. C. Wu, *Phys. Rev. B* **49**, 5034 (1994).

¹¹D. Wu, D. Fu, H. Guo, Z. Zhang, X. Meng, and X. Fan, *Phys. Rev. B* **56**, 4949 (1997).

¹²S. Lopez, H. M. Dunlop, M. Benmalek, G. Tourillon, M. S. Wong, and W. D. Sproul, *Surf. Interface Anal.* **25**, 315 (1997).

¹³H. Sjöstrom, S. Stafstrom, M. Boman, and J. E. Sundgren, *Phys. Rev. Lett.* **75**, 1336 (1995).

¹⁴D. Marton, K. J. Boyd, A. H. Al-Bayati, S. S. Todorov, and J. W.

- Rabalais, Phys. Rev. Lett. **73**, 118 (1994).
- ¹⁵K. J. Boyd, D. Marton, S. S. Todorov, A. H. Al-Bayati, J. Kulik, R. A. Zuhr, and J. W. Rabalais, J. Vac. Sci. Technol. A **13**, 2110 (1995).
- ¹⁶Z. F. Ren, Z. P. Huang, J. W. Xu, J. H. Wang, P. Bush, M. P. Siegal, and P. N. Provencio, Science **282**, 1105 (1998).
- ¹⁷H. Xin, C. Lin, W. P. Xu, L. Wang, S. Zou, X. Wu, X. Shi, and H. Zhu, J. Appl. Phys. **79**, 2364 (1996).
- ¹⁸S. Matsumoto, E. Q. Xie, and F. Izumi, Diamond Relat. Mater. **8**, 117 (1999).
- ¹⁹C. Ronning, H. Feldermann, R. Merk, H. Hofsass, P. Reinke, and J. U. Thiele, Phys. Rev. B **58**, 2207 (1998).
- ²⁰C. Fuchs, R. Henck, E. Fogarassy, J. Hommet, and F. Le Normand, J. Phys. IV **9**, 145 (1999).
- ²¹T. Szörényi, C. Fuchs, E. Fogarassy, J. Hommet, and F. Le Normand, Surf. Coat. Technol. **125**, 308 (2000).
- ²²T. Szörényi, E. Fogarassy, C. Fuchs, J. Hommet, and F. Le Normand, Appl. Phys. A: Mater. Sci. Process. **69**, S94 (1999).
- ²³M. P. Seah, in *Practical Surface Analysis by Auger and XPS*, edited by D. Briggs and M. P. Seah (Wiley, Chichester, U.K., 1983).
- ²⁴J. H. Scofield, J. Electron Spectrosc. Relat. Phenom. **8**, 129 (1976).
- ²⁵S. Tanuma, C. J. Powell, and D. R. Penn, Surf. Interface Anal. **11**, 577 (1988).
- ²⁶H. Froitzheim, in *Electron Spectroscopy for Surface Analysis*, edited by H. Ibach (Springer, Berlin, 1977), p. 205.
- ²⁷P. M. A. Sherwood, in *Practical Surface Analysis by Auger and XPS*, edited by D. Briggs and M. P. Seah (Wiley, Chichester, U.K., 1983), p. 44.
- ²⁸A. F. Wells, in *Structural Inorganic Chemistry* (Oxford, London, 1982), p. 832.
- ²⁹L. Constant and F. Le Normand (to be published).
- ³⁰G. Beamson and D. Briggs, in *High Resolution XPS on Organic Compounds* (Wiley, Chichester, U.K., 1992), p. 84.
- ³¹J. Mulder, in *Handbook of X-Ray Photoelectron Spectroscopy* (Perkin Elmer, Eden Prairie, 1982), p. 147.
- ³²J. Schafer, J. Ristein, R. Graupner, L. Ley, U. Stephan, Th. Frauenheim, V. S. Veerasamy, G. A. J. Amaratunga, M. Weiler, and H. Ehrhardt, Phys. Rev. B **53**, 7762 (1996).
- ³³M. Cardona and L. Ley, in *Photoemission in Solids I*, edited by M. Cardona and L. Ley (Springer, Berlin, 1978), p. 60.
- ³⁴W. F. Egelhoff Jr., Surf. Sci. Rep. **6**, 323 (1986).
- ³⁵R. Graupner, F. Maier, J. Ristein, L. Ley, and Ch. Jung, Phys. Rev. B **57**, 123 97 (1998).
- ³⁶L. Pauling, in *The Nature of the Chemical Bond*, 2nd ed. (Butterworths, London, 1958).
- ³⁷S. Muhl and J. M. Mendez, Diamond Relat. Mater. **8**, 1809 (1999), and references therein.
- ³⁸C. S. Cojocar and F. Le Normand (unpublished).
- ³⁹Z. J. Zhang, S. Fan, J. Huang, and C. M. Lieber, J. Electron. Mater. **25**, 57 (1996).
- ⁴⁰I. Bertóti, M. Mohai, A. Toth, and B. Zelei, Nuclear Inst. Meth. B **148**, 645 (1999).
- ⁴¹J. P. Boutique, J. J. Verbiest, J. G. Fripiat, J. Delhalle, G. Pfister-Guillouzo, and G. J. Ashwell, J. Am. Chem. Soc. **106**, 4374 (1984).
- ⁴²H. K. Woo, Y. Zhang, S. T. Lee, C. S. Lee, Y. W. Lam, and K. W. Wong, Diamond Relat. Mater. **6**, 635 (1997).
- ⁴³S. Matsumoto, K. K. Chattopadhyay, M. Mieno, and T. Ando, J. Mater. Res. **13**, 180 (1998).
- ⁴⁴J. M. Ripalda, E. Roman, N. Diaz, L. Galan, I. Montero, G. Comelli, A. Baraldi, S. Lizzit, A. Goldoni, and G. Paolucci, Phys. Rev. B **60**, R3705 (1999).
- ⁴⁵F. Weich, J. Widany, and T. Frauenheim, Phys. Rev. Lett. **78**, 3326 (1997).
- ⁴⁶E. Gyorgy, I. N. Mihailescu, L. Baleva, E. P. Trifonova, A. Zocco, and A. Perrone, Thin Solid Films (to be published, 2000).